Chapter 4
Fatigue Properties Assessment of API 5L Gr. B Pipeline Steel Using Infrared Thermography

V. E. L. Paiva, R. D. Vieira, and J. L. F. Freire

Abstract Simple and fast procedures to measure the fatigue limit using infrared thermography were proposed in the literature in the last two decades ago. In general, they consider fatigue damage as an energy dissipation process that is accompanied by some temperature variation ΔT. Those procedures significantly reduce fatigue testing costs by decreasing the quantity of required specimens and by shortening the testing time. The aim of the present work is to evaluate the fatigue limit, the stress amplitude vs. number of cycles fatigue (S-N) curve, and the influence of mean stress on the fatigue strength. Pipeline steel API 5L Gr. B, very common in the pipeline industry, was the test material. Uniaxial tensile specimens were tested under quasi-static monotonic load or under cyclic loads for different minimum to maximum load ratios. During each test, the surface temperature of the specimens was recorded in real time by a microbolometer thermocamera.

Keywords Infrared · Thermography · Fatigue · Damage · Pipeline material

4.1 Introduction

Two simple procedures to measure the fatigue limit using infrared IR thermography were proposed by Risitano and co-workers [1–4]. In [1–3], uniaxial tensile specimens are subjected to cyclic axial loading. In [4], the initiation of plasticity behavior is captured by the temperature measurements performed during a monotonic quasi-static tensile test to determine the material fatigue strength for full alternated cyclic load ratio (R = min load/max load = −1). The so called Ristano's rapid fatigue assessment procedure encounter other well developed similar approaches, as for example, by Luong [5], Krapez and Pacou [6] and de Finis et al. [7]. The cyclic and quasi-static rapid assessment of the fatigue limit consider the fatigue damage as an energy dissipation process that is accompanied by some temperature variation ΔT. In the general cyclic procedure a test specimen is subjected to a number of blocks of constant stress amplitude loading cycles, which are gradually increased until they eventually cause failure. The quasi-static method is based on the first deviation of the slop of the temperature curve that occurs in the uniaxial tension test. The uniaxial stress value related to the slope deviation point is the full alternate fatigue strength, valid for $R = -1$. Both methods significantly reduce the traditional fatigue testing costs by decreasing the quantity of required specimens and by shortening the testing time. The aim of the present work is to evaluate the fatigue limit, the stress amplitude vs. number of cycles fatigue (S-N) curve, and the influence of mean stress on the fatigue strength. Pipeline steel API 5L Gr. B, very common in the pipeline industry, was the test material.

4.2 Material and Experimental Procedure

Uniaxial specimens were tested in a 100 kN INSTRON servo-hydraulic machine under quasi-static monotonic load or cyclic axial load. The stroke rate applied in the static tests was 1 mm/min. Based on the cyclic experimental methodology proposed, the cyclic tests employed stepped loading cycles, sequentially applied to each specimen at a constant amplitude force-control, with 5–15 Hz frequency and varying load ratios R. During each quasi-static or cyclic test, the surface temperature of the specimen was recorded in real time by a microbolometer thermocamera FLIR A655sc (640 × 480 uncooled microbolometers, 50 Hz acquisition rate, 17 μm spatial resolution, 30 mK sensitivity). The temperature data was acquired and analyzed using the ResearchIR software from FLIR.

V. E. L. Paiva · R. D. Vieira · J. L. F. Freire (✉)
Pontifical Catholic University of Rio de Janeiro, PUC-Rio, Rio de Janeiro, Gávea, RJ, Brazil
e-mail: jlfreire@puc-rio.br

A. Baldi et al. (eds.), *Residual Stress, Thermomechanics & Infrared Imaging, Hybrid Techniques and Inverse Problems, Volume 7*,
Conference Proceedings of the Society for Experimental Mechanics Series, https://doi.org/10.1007/978-3-319-95074-7_4

Table 4.1 Material properties

Chemical composition	0.15C, 0.83Mn, 0.19Si, 0.02P, 0.003S
Yield strength S_y (average of 3 specimens)	316 MPa (0.5% total engineering strain)
Ultimate strength S_u (average of 3 specimens)	420 MPa

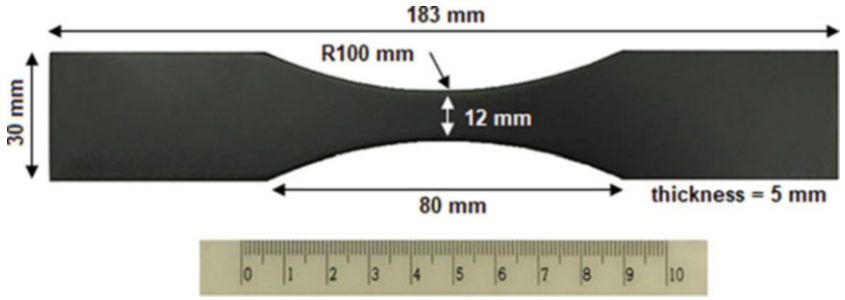

Fig. 4.1 Specimen's geometry

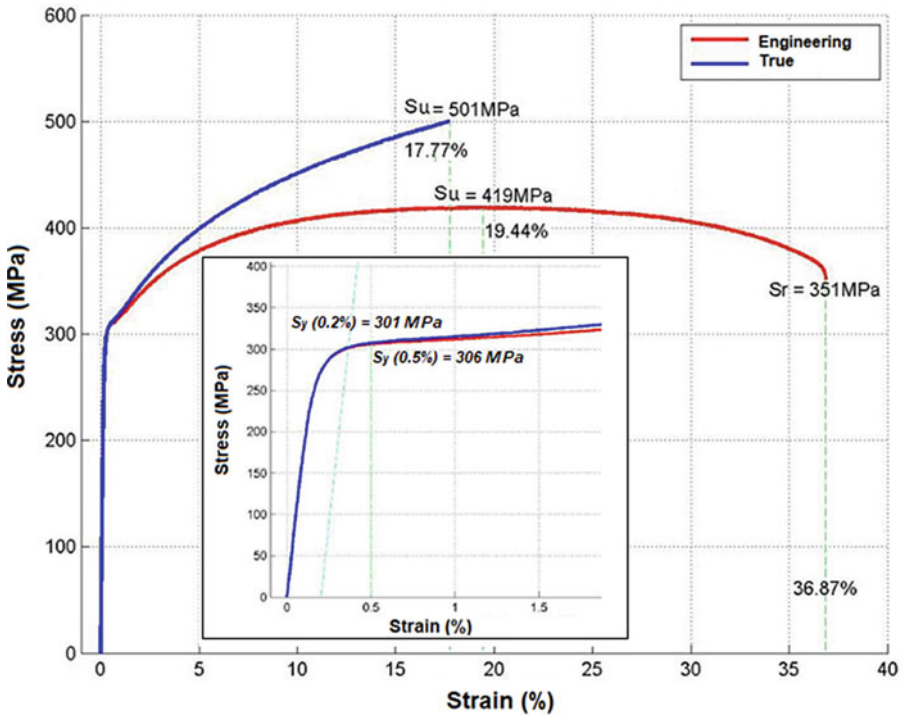

Fig. 4.2 Tensile stress-strain curve of one of the 3 specimens of API 5L Gr. B pipe

Relevant material data are given in Table 4.1. The uniaxial test specimens were machined from longitudinal strips cut from a thin walled API 5L Gr. B pipe having a nominal outside diameter D = 324 mm and thickness t = 6.35 mm. Figure 4.1 gives the final nominal specimen's dimensions following ASTM E 466. All uniaxial specimens were painted with a thin layer of opaque black paint to increase emissivity. The uniaxial tensile stress-strain curve for the pipe material is given in Fig. 4.2.

4.3 IR Thermography

According to the methodology proposed in [1–3], when the specimen is loaded below the fatigue limit, its temperature varies very slightly, but for alternated stress amplitudes ($\Delta\sigma_i = \sigma_{ai}$) above the fatigue limit the temperature variations are significant. The temperature variation according to a given reference (ΔT) may be classified along the test inside three

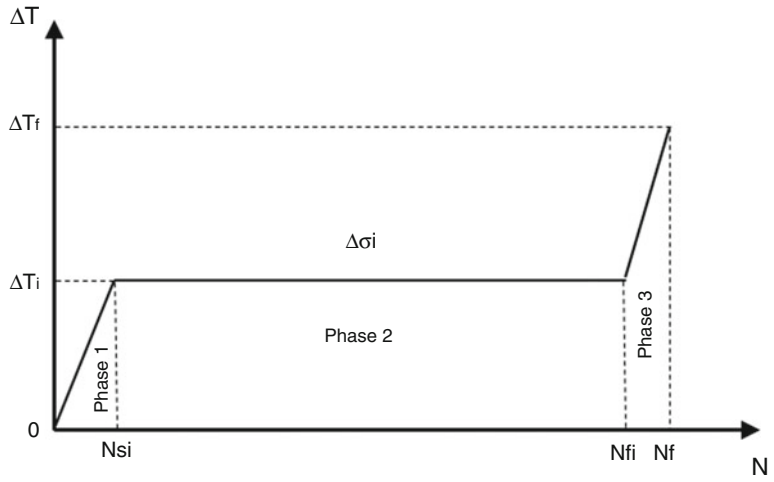

Fig. 4.3 Phases of the thermal behavior of ΔT vs. N curve for a hot spot in the specimen surface during typical fatigue tests. (Adapted from Ref. [2])

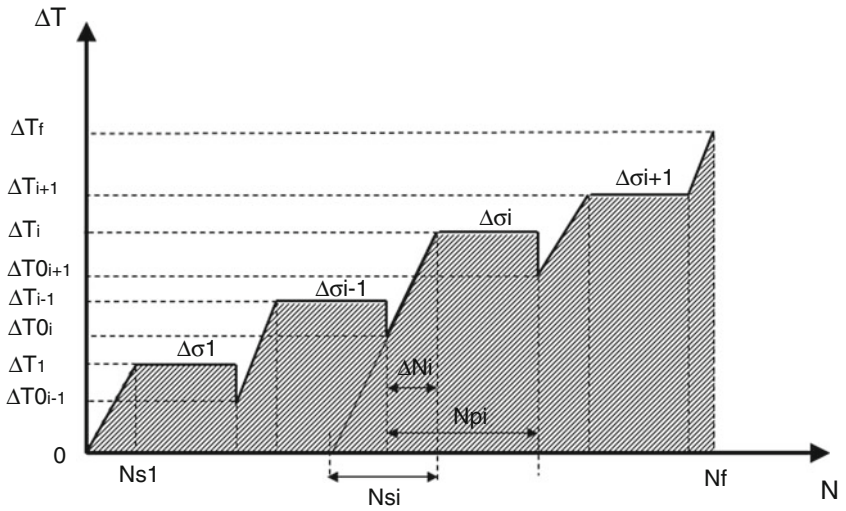

Fig. 4.4 Stepped loading procedure for the determination of the fatigue limit and the integral ϕ

phases. Figure 4.3 presents the temperature variation with the number of cycles N for the test where the stress amplitude $\Delta\sigma_i$ was made constant. They increase during the first part of the test (phase 1), then remain stable for a while (phase 2), and finally rapidly increase prior to failure at a life of N_f cycles (phase 3), as shown in Fig. 4.3.

Through the analysis of the temperature response curve under incremental cyclic step loading, see Figs. 4.4 and 4.5a, b, the fatigue limit can be evaluated. Each stress amplitude level corresponds to one stabilization temperature. Two linear regression lines are used to approximate the thermal data and to determine graphically the fatigue limit, as depicted in Fig. 4.5b. The first line contains the data where the applied stress is below the fatigue limit, and the second line fits the data located above the limit. The fatigue limit is determined by the intersection of these two lines, as shown in Fig. 4.5b.

Using the same line of analysis, Fargione et al. [2] proposed a method to determine the fatigue-life curve S-N of the material using IR thermography. This method is much faster than the traditional one and needs theoretically only one specimen. In practice, the recommended minimum number of specimens is three. For small temperature variations (under 100 K, implicating small loading frequencies), the heat transferred from the specimen to the environment can be considered proportional to the temperature difference ΔT. A parameter ϕ, which is the integral of the ΔT vs. N curve in Fig. 4.3, Eq. (4.1),

$$\phi = \int_0^{N_f} \Delta T \, dN \tag{4.1}$$

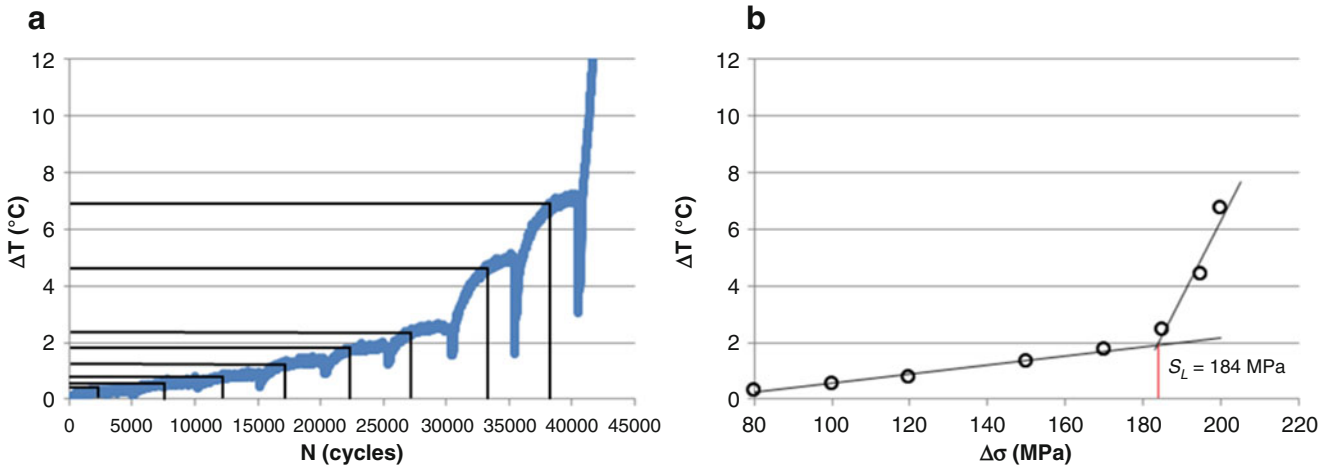

Fig. 4.5 (**a**) ΔT vs. N curve for various stress amplitudes $\Delta\sigma_i$, with the determination of each ΔT_i. (**b**) ΔT_i vs. $\Delta\sigma_i$ curve for various incremental load steps and determination of the fatigue limit (intercept of the two straight lines). Data obtained for specimen 2 of the present paper, $R = 0.025$

is assumed constant for given test conditions, such as the specimen geometry and material, loading frequency and environment. This critical value corresponds to fatigue failure and it is associated to the total area under the curve of Fig. 4.3 (for one constant stress amplitude level), or the total dashed area in Fig. 4.4 (for several stress amplitude levels). The ϕ value can be used together with values of ΔT_i, ΔT_{0i}, ΔN_i measured at stress amplitude levels $\Delta\sigma_i$ for a single specimen, as depicted in Fig. 4.3 and modeled by Eqs. (4.2) and (4.3), to yield the whole fatigue S-N curve. Each data point of the S-N curve is formed by the pair (N_{fi}, $\Delta\sigma_i$) where N_{fi} is calculated from Eq. (4.2). This equation is derived with the help of Fig. 4.4 and the assumption that phase 3, depicted in Fig. 4.3, is small and can be neglected. The value of N_{si} is determined from Eq. 4.3 with the help of Fig. 4.4.

$$\phi = \Delta T_i \left(N_{fi} - \frac{\Delta N_{si}}{2} \right) \tag{4.2}$$

$$N_{si} = \frac{\Delta N_i \, \Delta T_i}{\Delta T_i - \Delta T_{0i}} \tag{4.3}$$

A partial damage value D_i results from the partial integrated value ϕ_i resulting from the application of each stress amplitude $\Delta\sigma_i$. The value ϕ_i is calculated considering the number of cycles applied at each stress level, N_{pi}. The denominator of Eq. (4.4) gives the area under the curve ΔT vs. N considering the interval N_{pi}. The partial damage value of Eq. (4.4) assumes that the Miner's linear damage accumulation rule is valid.

$$D_i = \frac{\phi_i}{\phi} = \frac{\left(\frac{\Delta T_i + \Delta T_{0i}}{2} \right) \Delta N_i + \Delta T_i \left(N_{fi} - \Delta N_{si} \right)}{\sum_1^f \phi_f} \tag{4.4}$$

Based on the experimental cyclic methodology [1–3], next section presents results for four specimens that were tested under a step loading procedure, sequentially applied to each specimen at a constant amplitude under force-control, with stress ratios $R = \sigma_{min}/\sigma_{max}$ equal to $R = 0.025$ and 0.5. At each load step, the load amplitude was maintained fixed during blocks of $5 \cdot 10^3$ cycles, a value that was high enough for the temperature to achieve a stable thermal behavior, as determined by preliminary tests. Afterwards, the load was increased until the specimen failed. One specimen was tested based on the quasi-static methodology [4]. Results from both cyclic and quasi-static analyses are presented in the next section.

4.4 Results and Discussion

Results of tests performed to characterize the uniaxial material behavior are given in Figs. 4.2, 4.5, 4.6, and 4.7 and reported in Tables 4.1, and 4.2. Figure 4.2 gives the uniaxial material stress-strain curve for a monotonic test. The detailed plot inside the larger plot shows the method used to determine the 0.5% yield strength for a longitudinal test specimen.

Figure 4.5 depicts the determination of the fatigue limit by applying the Risitano's rapid method [1–3]. The temperature variation with number of cycles and with applied stress amplitude are presented respectively in Fig. 4.5a, b. These plots show that the temperature undergoes a significant increase when it is submitted to elevated stress levels, above the fatigue limit. Figure 4.5a shows that temperature stabilizes around 2300 cycles for each stress level, completing the transition from phase 1 to phase 2, as showed in Fig. 4.3. Figure 4.5a shows that, after reaching temperature stabilization, the cyclic loading is kept for approximately 2700 cycles until the test stress level is changed. This way the specimen is consecutively loaded until it finally reaches its failure (phase 3 in Fig. 4.3).

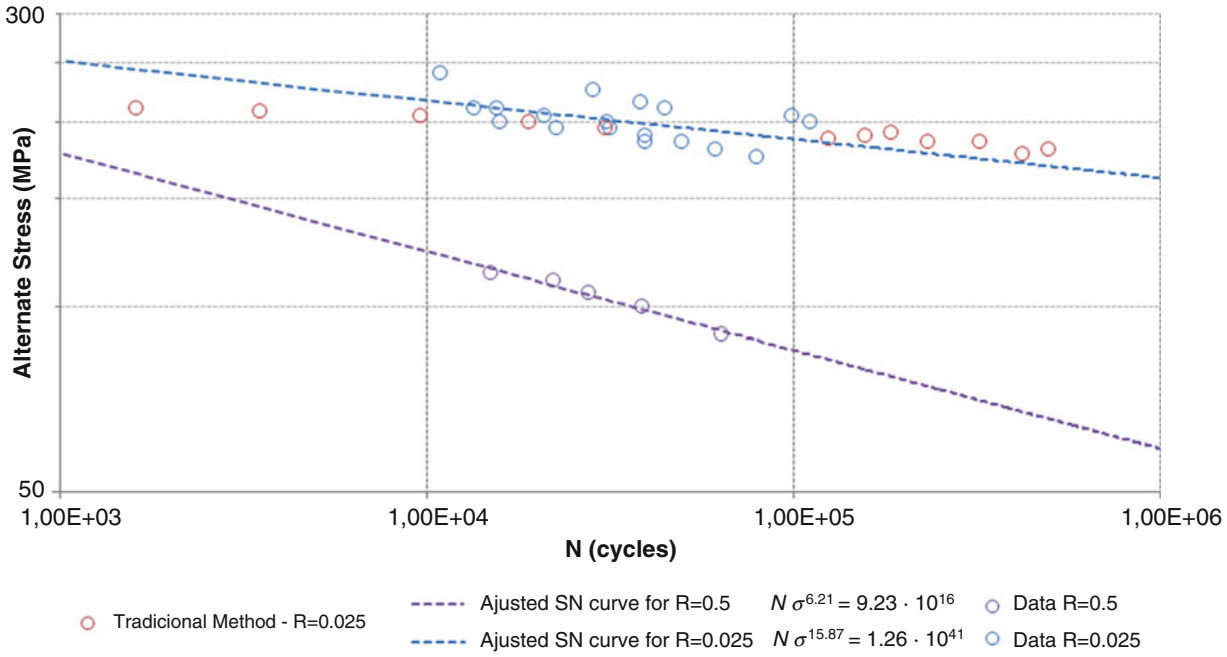

Fig. 4.6 Fatigue *S-N* curve for stress ratios $R = 0.025$ and $R = 0.5$

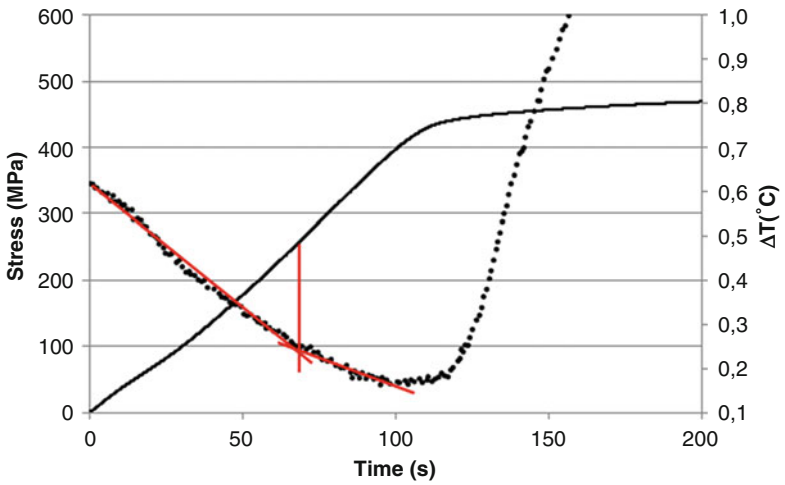

Fig. 4.7 Fatigue limit ($R = -1$) for steel API 5 L Gr. B using the quasi-static method proposed in [4]

Table 4.2 Measured results for each specimen

Specimen	Fatigue limit S_L (MPa)	R	Frequency (Hz)	Test type	ϕ (°C·cycles)	D (from Eq. (4.4))
1	169	0.025	15	Cyclic	1.53×10^5	0.98
2	184	0.025	15		9.2×10^4	0.97
3	86	0.5	15		3.0×10^4	0.96
6	196	0.025	5		5.2×10^5	0.95
5	253	−1	1 mm/min stroke	Quasi-static	–	–

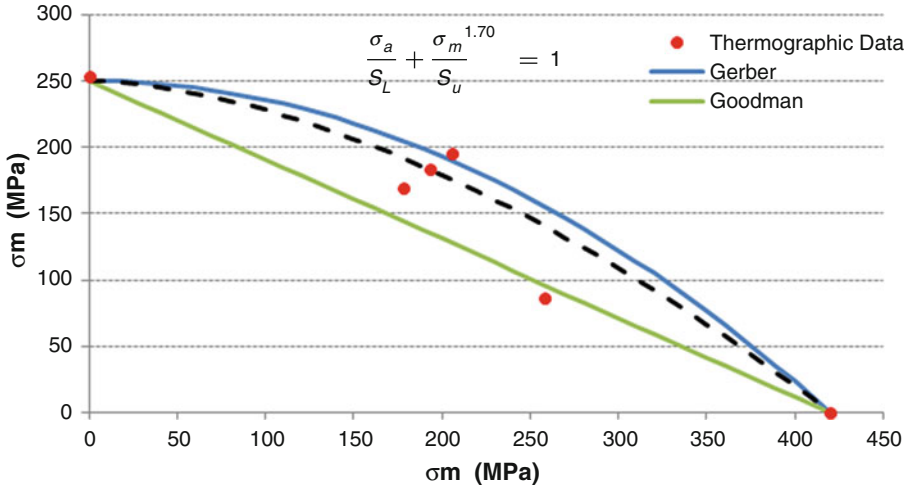

Fig. 4.8 Plot for alternate stress vs. mean stress for Gerber and Goodman lines and for thermographic data

Figure 4.5b shows the stabilized temperatures, ΔT_i, obtained from Fig. 4.5a, plotted against their corresponding amplitude stress levels, $\Delta\sigma_i$. According to Ristanos' method, the fatigue limit S_L can be determined graphically by the intersection of two regression lines based on the data below and above the fatigue limit, as illustrated in Fig. 4.5b. When the specimen is subjected to a stress amplitude above the fatigue limit, its temperature increases significantly and damage begins to accumulate at one or more critical hotspots until the formation and propagation of a crack that leads to the specimen failure. Figure 4.5b shows the fatigue limit $S_L = 184$ MPa determined for specimen 2 under $R = 0.025$. Values for other specimens tested under ratios R equal to 0.025 and 0.5 are given in Table 4.2.

Having determined the values of ϕ as presented in Eq. (4.2), the S-N fatigue curve can be determined using the process outlined in the previous section. The S-N fatigue curves for each stress ratio R calculated in this way are presented in Fig. 4.6. The calculated curves encompass data fitted to the interval 10^3 to 10^6 cycles. Traditional fatigue tests were also performed using the ratio $R = 0.025$ and are plotted in Fig. 4.6. Table 4.2 presents the fatigue results for all tested specimens using the rapid assessment method.

Figure 4.7 depicts the quasi-static determination of the full alternated uniaxial fatigue limit of the pipe material as proposed by Risitano et al. [4]. The method is based on the first deviation of the slop of the temperature curve that occurs in the uniaxial tension test. This slope deviation point is related with the fully alternate fatigue strength, valid for $R = -1$. This value was found to be $S_{L\_R=-1} = 253$ MPa.

It is interesting to note that the results for $R = -1$ (from the static test), $R = 0.025$ and $R = 0.5$ (from the cyclic tests), together with the material ultimate strength S_u, are compatible with the mean stress influence on the fatigue limit when seen under the light of a plot of alternated vs. mean stress, presented in Fig. 4.8. In this Figure, Goodman and Gerber curves, computed using the values of $S_L = 253$ MPa for $R = -1$ and $S_u = 420$ MPa, are plotted for comparison purpose. Similar results have already been published by Krapez and Pacou [6] for steel X48 and Rego et al. [8] for brass 36,000.

Based on the fatigue limits presented in Table 4.2 for each applied R, data points formed by pairs of alternate stress amplitude values (σ_a) and mean stress (σ_m) were calculated and plotted in Fig. 4.8. The resulting data was adjusted by a parabolic fitting equation presented in Eq. (4.5), the adjusting exponent α being equal to 1.70. This exponent falls between the exponents given by the so called Goodman and Gerber curves, respectively equal to 1 and 2 [9].

$$\frac{\sigma_a}{S_L} + \left(\frac{\sigma_m}{S_u}\right)^{\alpha} = 1 \tag{4.5}$$

4.5 Conclusions

This paper confirms that rapid fatigue damage assessment methods are practical and efficient tools that can provide a reliable and fast way to determine the fatigue behavior of materials using few specimens. More specifically, the paper furnishes fatigue data for the API 5L Gr. B pipeline steel, which is scarce in the literature. Moreover, the influence of the stress ratio R was evaluated for this material and an equation showing the influence of the mean applied stress on the fatigue limit was given, which can be useful for design purpose.

References

1. La Rosa, G., Risitano, A.: Thermographic methodology for rapid determination of the fatigue limit of materials and mechanical components. Int. J. Fatigue. **22**, 65–73 (2000)
2. Fargione, G., Geraci, A., La Rosa, G., Risitano, A.: Rapid determination of the fatigue curve by the thermographic method. Int. J. Fatigue. **24**, 11–19 (2000)
3. Risitano, A., Risitano, G.: Cumulative damage evaluation of steel fracture mechanics. Theor. Appl. Fract. Mech. **54**, 82–90 (2010)
4. Risitano, G., Risitano, A., Clienti, C.: Determination of the fatigue limit by semi static tests. Convegno Nationale, IGF XXI, Cassino, Italia 13–15 Giugo 2011, pp. 322–330
5. Luong, N.P.: Infrared thermography of fatigue in metals. SPIE vol 1682 Thermosense XIV
6. Krapez, J.C., Pacou, D.: Thermographic detection of damage initiation during fatigue tests. SPIE vol 4710 2002 Thermosense XXIV
7. de Finis, R., Palumbo, D., Ancona, F., Galietti, U.: Fatigue limit evaluation of various martensitic stainless with new robust thermographic data analysis. Int. J. Fatigue. **74**, 88–96 (2015)
8. Rego, L.L.L., Castro, J.T.P., Freire, J.L.F., Paiva, V.E.L.: Fatigue characterization of the C36000 copper alloy using the thermographic method. In: 24th ABCM International Congress of Mechanical Engineering, 3–8 Dec, 2017, Curitiba
9. Castro, J.T.P., Meggiolaro, M.A.: Fatigue Design Techniques, Volume 1: High-Cycle Fatigue. CreateSpace Independent Publishing Platform (2016)